Absence of superconductivity in hole-doped $BaFe_{2-x}Cr_xAs_2$ single crystals

Athena S. Sefat,[1] David J. Singh,[1] Lindsay H. VanBebber,[2] Yurij Mozharivskyj,[3] Michael A. McGuire,[1] Rongying Jin,[1] Brian C. Sales,[1] Veerle Keppens,[2] and David Mandrus[1]

[1]*Materials Science and Technology Division, Oak Ridge National Laboratory, Oak Ridge, Tennessee 37831-6114, USA*

[2]*Department of Materials Science and Engineering, University of Tennessee, Knoxville, Tennessee 37996-2200, USA*

[3]*Department of Chemistry, McMaster University, Hamilton, Ontario, Canada L8S 4M1*

(Received 2 April 2009; revised manuscript received 28 May 2009; published 19 June 2009)

We investigate the physical properties and electronic structure upon Cr doping in the iron arsenide layers of $BaFe_2As_2$. This form of hole doping leads to suppression of the magnetic/structural phase transition in $BaFe_{2-x}Cr_xAs_2$ for $x>0$, but does not lead to superconductivity. For $x\leq 0.75$ values, temperature dependence of the resistivity, specific heat, magnetic susceptibility, Hall coefficient, and single-crystal x-ray diffraction data are presented. The resulting phase diagram is suggestive that superconductivity does not derive simply from the suppression of the structural/magnetic transitions. The materials show signatures of approaching a ferromagnetic state for x as little as 0.36 by an enhanced Wilson ratio. Such results reflect renormalization due to spin fluctuations and they are supported by density-functional supercell calculations for slightly higher doping level of $x=1$. Calculations show a strong interplay between magnetic ordering and chemical ordering of Fe and Cr, with a ferromagnetic ground state.

DOI: 10.1103/PhysRevB.79.224524 PACS number(s): 75.30.−m, 71.20.−b

I. INTRODUCTION

The discovery of high-T_C superconductivity in the Fe-based systems has attracted great interest primarily due to their non copper-based origin. The structural parents of such superconductors include those of tetragonal $ThCr_2Si_2$-type AFe_2As_2,[1] the so-called "122" family. The stoichiometric compounds exhibit an antiferromagnetic spin-density-wave ordering of Fe spins at 171 K in $A=$Ca,[2] 205 K in $A=$Sr,[3] 132 K or 140 K in $A=$Ba,[4,5] and at 200 K in $A=$Eu,[6] likely coupled with a structural transition. The onset of superconductivity in 122 family with suppression of the magnetic ordered state is similar to the behavior observed in the cuprates and can be induced by applying pressure,[7] hole doping on the A site,[8] or electron doping on the Fe site.[9] The appearance of superconductivity is associated with the suppression of the structural/magnetic phase transitions. The induced superconductivity due to in-plane cobalt doping provides one crucial distinction from the cuprates.[9] In addition, the itinerant and weakly correlated electrons in AFe_2As_2 parents distinguish them from the cuprate Mott-insulating parents. Here we investigate the properties of $Ba(Fe,Cr)_2As_2$ solid solution by hole doping in the FeAs layers of $BaFe_2As_2$. This system allows the exploration of the structural/magnetic phase transitions and its possible relation to superconductivity. Compared to Fe^{2+} ion ($3d^6$), Cr^{2+} has two less $3d$ electrons. Thus it is expected that Cr doping introduces disorder in the iron arsenide layer, and changes both crystal and electronic structures. The crystallographic and electronic structure, and thermodynamic and transport properties of Cr-doped $BaFe_2As_2$ crystals are presented.

While for undoped $BaFe_2As_2$ a single structural/magnetic transition is observed at $T_N=132(1)$ K in specific heat,[4,5] for $x=0.04$, the transition is shifted to 116 K. Much to our surprise, single-crystal x-ray diffraction data at 100 K gives a volume change but no detectable symmetry-breaking transition for this composition. With more Cr substitution in $BaFe_{2-x}Cr_xAs_2$, the magnetic transition temperature continues to decrease. For $x=0.75$, there is no evidence of long-range magnetic order, nor superconductivity down to 1.8 K. Theory suggests that $BaCr_2As_2$ is an itinerant antiferromagnetic metal.[10] The stronger Cr-As covalency relative to $BaFe_2As_2$ may explain why superconductivity is not observed in Cr-doped $BaFe_2As_2$. Large single crystals of $BaFe_{2-x}Cr_xAs_2$ with $0\leq x\leq 0.75$ are grown to study the systematic property changes.

II. RESULTS AND DISCUSSION

The single crystals of $BaFe_{2-x}Cr_xAs_2$ were grown out of a mixture of FeAs and CrAs flux. High purity elements (>99.9%, from Alfa Aesar) were used in their preparations. The FeAs and CrAs binaries were synthesized similarly to our recent report.[9] To produce a sample with a nominal composition (x_{nomin}) of 0.06, a ratio of Ba:FeAs:CrAs $=1:4.85:0.15$ was used; for $x_{nomin}=0.12$, this ratio was 1:4.7:0.3; for $x_{nomin}=0.22$, this ratio was 1:4.45:0.55. Each of these mixtures was heated in an alumina crucible for 13 h at 1230 °C under a partial atmosphere of argon. Each reaction was then cooled at a rate of 1.8 °C/h, followed by decanting the FeAs/CrAs flux at 1100 °C. In order to produce a sample with $x_{nomin}=0.14$, a ratio of Ba:FeAs:CrAs=1:4.3:0.7 was used; for $x=0.28$, this ratio was 1:3.6:1.4; for $x_{nomin}=0.5$, this ratio was 1:3.75:1.25; for $x_{nomin}=1$, this ratio was 1:2.5:2.5. Each of these mixtures was heated for 10 h at 1230 °C and then cooled at a rate of 2 °C/h, followed by the decanting of the flux at 1120 °C. The crystals had sheet morphologies and dimensions of $\sim 6\times 5\times 0.15$ mm^3 or smaller in a, b, and c directions, respectively. Similar to $BaFe_2As_2$,[9] the crystals formed with the [001] direction perpendicular to the plane of the plates. Attempts of crystal growth for $x_{nominal}>1.0$ values were unsuccessful, but may be possible by revisiting the synthetic routes.

TABLE I. Chemical composition and lattice constants of $BaFe_{2-x}Cr_xAs_2$ found at room temperature. The lattice constants are determined from powder x-ray diffraction analyses.

Nominal Fe:Cr	Microprobe Fe:Cr x (± 0.02)	c (Å)	a (Å)
2:0	2:0	13.018(1)	3.9642(3)
1.94:0.06	1.96:0.04	13.040(1)	3.9620(3)
1.88:0.12	1.92:0.08	13.064(2)	3.9631(4)
1.78:0.22	1.86:0.14	13.085(2)	3.9618(4)
1.72:0.28	1.80:0.20	13.112(1)	3.9665(3)
1.68:0.32	1.77:0.23	13.120(2)	3.9601(3)
1.5:0.5	1.64:0.36	13.165(2)	3.9657(3)
1:1	1.25:0.75	13.260(1)	3.9792(3)
0:2	0:2	13.632(3)	3.9678(5)

The chemical composition was measured with a JEOL JSM-840 scanning electron microscope, same as that described in Ref. 9. Energy-dispersive x-ray spectroscopy (EDS) analyses indicated that less Cr was substituted in the crystal than put in solution; these results are summarized in Table I. Three spots were checked on the surface of each single crystal, and no impurity phases were detected. The samples will be denoted by these measured values of x throughout this paper.

The phase purity of the crystals was characterized using a Scintag XDS 2000 powder x-ray diffractometer. Lattice constants were determined from full-pattern LeBail refinements using the program FULLPROF.[11] At room temperature the structures are identified as the tetragonal $ThCr_2Si_2$ ($I4/mmm$, $Z=2$). Table I gives the refined lattice constants from powder x-ray diffraction; Fig. 1 plots a and c parameters as a function of Cr concentration. The incorporation of $x=0.75$ Cr in the Fe site increases the cell volume by 2.6%, mainly due to the increase in the c lattice constant. Single-crystal x-ray diffraction was also done at room temperature for $x=0.75$. Analysis of the diffraction spots of the crystals indicated that there were multiple domains (plates with a preferred stacking) giving some smeared reflections. The refined lattice parameters are $a=3.985(3)$ and $c=13.277(17)$ Å, similar to powder x-ray diffraction results (Table I). Due to similarities between the Fe and Cr atomic scattering powers, the Fe/Cr ratios could not be refined.

Low-temperature single-crystal x-ray diffraction data was collected on the parent $BaFe_2As_2$. The crystal was placed under a stream of nitrogen gas and the data were collected on a Bruker Apex II diffractometer, first at 100 K. The refinement of the reflections gives the orthorhombic F-centered cell ($Fmmm$), as reported.[5] The refined lattice parameters are $a=5.595(3)$ Å, $b=5.610(3)$ Å, and $c=12.964(6)$ Å. The crystal was then warmed to 173 K; this structure was found to be tetragonal ($I4/mmm$) with lattice parameters of $a=3.9708(16)$ Å and $c=13.006(5)$ Å, as expected.

For small Cr-doping of $x=0.04$, low-temperature structure was also examined by single-crystal x-ray diffraction (Table II). A crystal was first examined at 100 K, then by warming to 117, 119, and finally 173 K. Surprisingly the 100 K structure refined in the tetragonal $I4/mmm$, with no sign of distortion. Shapes of several diffraction spots from 100 and 173 K were compared and they are almost identical. Also, the thermal ellipsoids are quite similar for 100 and 173 K in the $I4/mmm$. A small amount of chromium dopant seems to suppress a symmetry-breaking structural transition in $BaFe_2As_2$. If there is any distortion to a lower symmetry, it is relatively small and undetectable from the single-crystal data. Figure 2 shows the lattice constants as a function of temperature for $x=0.04$. There is an indication that some structural change may happen below 119 K since both cell parameters decrease. High-resolution powder diffraction may reveal peak splitting (orthorhombic or another distortion) if present. If a symmetry lowering does not occur, the concomitant decrease in both a and c suggest that the structural transition may be volumetric in nature.

Magnetic measurements were performed with a Quantum Design (Magnetic Property Measurement System) superconducting quantum interference device (SQUID) magnetometer. For a temperature-sweep experiment, the sample was cooled to 1.8 K in zero field (zfc) and data were collected by warming from 1.8 to 300 K in an applied field of 1 T. The magnetic-susceptibility results are presented per mole of formula unit (cm^3/mol), χ, along c- and ab-crystallographic directions [Figs. 2(a) and 2(b). For $BaFe_2As_2$ at room-temperature $\chi_c \approx \chi_{ab} \approx 6.5\times10^{-4}$ $cm^3\,mol^{-1}$, and the susceptibility decreases linearly with decreasing temperature, and drops abruptly below $T_N \approx 132$ K with $\chi_c > \chi_{ab}$. With Cr doping, the magnitude of the magnetic susceptibility increases at room temperature while the transition for magnetic order (probably T_N) decreases. At 1.8 K and for $x \leq 0.14$, χ_c is approximately 1.2 times larger than χ_{ab}. With more Cr

TABLE II. Crystal and structure data parameters for $x=0.04$ in $BaFe_{2-x}Cr_xAs_2$ ($\lambda=0.71073$ Å).

Temp. (K)	293(2)	173(2)	119(2)	117(2)	100(2)
Crystal system			Tetragonal		
Space group (no.), Z			$I4/mmm$ (139), 2		
a (Å)	3.970(2)	3.964(2)	3.967(2)	3.962(2)	3.954(2)
c (Å)	13.022(10)	13.002(11)	12.999(11)	12.984(10)	12.963(10)
V (Å^3)	205.2(2)	204.3(2)	204.6(2)	203.84(19)	202.7(2)
$d_{calc.}$ (Mg/m^3)	6.454	6.483	6.474	6.499	6.536
Final R_1, wR_2 [$I>2\sigma(I)$]	0.0295, 0.0565	0.0226, 0.0421	0.0263, 0.0459	0.0273, 0.0504	0.0281, 0.0468
Largest diff. peak and hole	1.65, −0.83	1.90, −1.05	2.32, −1.64	2.11, −1.13	2.78, −1.29

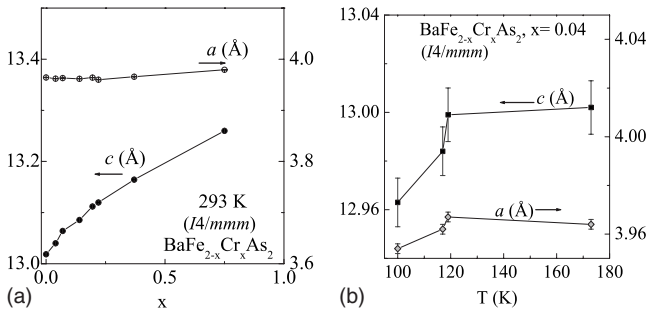

FIG. 1. (a) Lattice parameters for $BaFe_{2-x}Cr_xAs_2$ compositions at room temperature, refined from powder x-ray diffraction data. (b) The change in lattice parameters with temperature for $x=0.04$ in $BaFe_{2-x}Cr_xAs_2$, refined in the tetragonal lattice.

doping, the susceptibility becomes more anisotropic: for $x=0.20$ the ratio of $\chi_c/\chi_a=1.4$ (at 1.8 K), and for $x=0.36$ it is $\chi_c/\chi_{ab}=1.8$ (at 1.8 K). The susceptibilities along both crystallographic axes roughly converge and are isotropic above $T_N=118$ K for $x=0.04$, $T_N=104$ K for $x=0.08$, $T_N=88$ K for $x=0.14$, $T_N=80$ K for $x=0.20$, and $T_N=58$ K for $x=0.36$. For $x=0.75$ and at ~120 K there is a drop in χ_c and a small kink in χ_{ab}. For this sample there is also a broad feature at ~30 K in χ_{ab}. For $x=0.75$, the magnetic anisotropy switches, with $\chi_{ab}/\chi_c \approx 2$ at 1.8 K. Figures 2(b) and 2(c) illustrate the field-dependent magnetization at 1.8 K. For samples with $x \leq 0.20$, the behavior is linear. For $x=0.36$ (M_{ab}) and $x=0.75$ (M_c), there are nonlinearities in magnetization suggestive of metamagnetic transitions. These were not pursued any further here, but will be the subject of future investigations.

Transport measurements were performed with a Quantum Design Physical Property Measurement System (PPMS). Electrical leads were attached to the sample using Dupont 4929 silver paste and resistivity measured in the *ab* plane [Fig. 3(a)]. The $\rho_{300\ K}$ values range from 0.3 to 0.8 mΩ cm, although their absolute values may suffer from the geometry factor estimations. Temperature-dependent electrical resistivity for $BaFe_2As_2$ decreases with decreasing temperature, and below ~132 K there is a sharp drop. For $x>0$, instead of a drop in ρ_{ab}, there are sharp upturns below 117 K for $x=0.04$, 104 K for $x=0.08$, 90 K for $x=0.14$, and 60 K for $x=0.36$. The temperature of the anomaly is clearly diminished with increasing x, with no evidence of superconductivity down to 1.8 K. The resistivity for $x=0.75$ sample is roughly temperature independent down to ~100 K, and rises below. The difference between the resistivity anomaly for $x=0$ and those of $0.04 \leq x \leq 0.36$ is probably associated with changes in the scattering and the decrease in the number of carriers. For Cr-doped samples, no thermal hystereses were observed.

The Hall coefficient (R_H) of $BaFe_2As_2$ is negative in the temperature region of 125–145 K, and shows a sharp decrease at the structural/magnetic transition near 134 K.[13] For $BaFe_{2-x}Cr_xAs_2$ and $x>0$, R_H was calculated from the antisymmetric part of the transverse voltage (perpendicular to the applied current) under magnetic field (±6 T) reversal at fixed temperature. Systematic changes in $R_H(T)$ are observed upon Cr substitution [Fig. 3(b)]. For $x=0.04$, R_H is negative

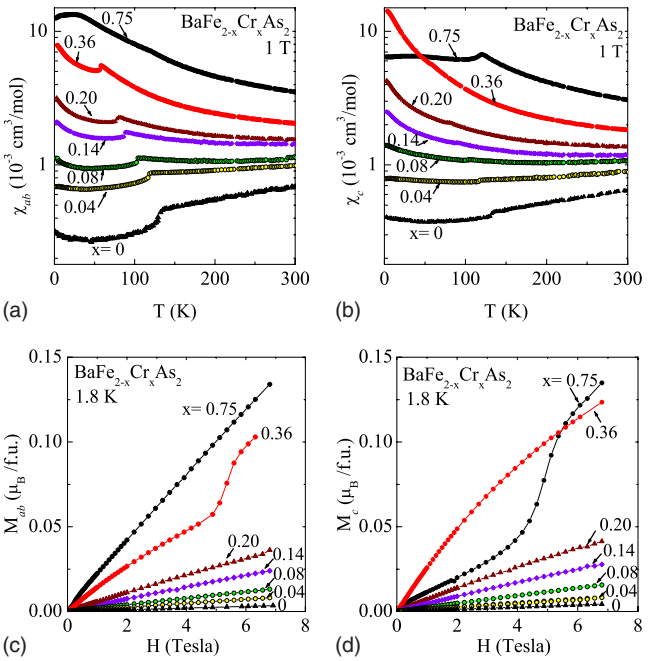

FIG. 2. (Color online) Temperature dependence of molar susceptibility for $BaFe_{2-x}Cr_xAs_2$ between $0 \leq x \leq 0.75$, along *ab*- (a) and *c*-lattice directions (b). Magnetization vs applied field measured at 1.8 K for $BaFe_{2-x}Cr_xAs_2$, along *ab*- (c) and *c*-lattice directions (d).

between 30 and 300 K, and becomes more negative with decrease in temperature, with a sharp anomaly at ~120 K similar to $BaFe_2As_2$.[13] R_H gives a minimum near 90 K for $x=0.04$, becoming less negative thereon and positive below 30 K. Qualitatively different behavior is observed at the phase transition for $x>0.04$. For $x=0.08$, $x=0.14$, and $x=0.36$, R_H displays an abrupt upturn upon cooling near 104, 90, and 60 K, respectively, and is approximately temperature independent at higher temperatures. These anomalies in R_H coincide with T_N observed in $\chi(T)$ and anomalies observed in $\rho(T)$. For $x=0.75$, R_H is roughly temperature independent and positive down to 5 K. The positive values observed at low temperatures in the lightly doped materials and the tendency of R_H toward more positive values with x at higher temperatures are indications that Cr acts as a hole dopant in $BaFe_2As_2$. More detailed analysis of R_H is complicated by the multiband nature of the system and the likely presence of both electron and hole bands at the Fermi level.

Specific heat data were collected on single crystals [Fig. 4(a)], also using a PPMS. For $BaFe_2As_2$, a transition is observed at 132(1) K, associated with a tetragonal to orthorhombic *Fmmm* distortion, and a spin-density wave (SDW) magnetic transition.[4,12] With Cr doping, the transition temperatures decrease. For $x=0.75$, there are no anomalies in specific heat down to 1.8 K [Fig. 4(a), inset]. Figure 4(b) plots the C/T versus T^2 dependence up to ~10 K. Although this region is not very linear, the Sommerfeld-coefficient γ may be estimated. For $BaFe_2As_2$, $\gamma=6.1$ mJ/(K^2 mol) [or 3.0 mJ/(K^2 mol Fe)].[12] The γ value increases consistently with Cr doping: $\gamma \approx 30$ mJ/(K^2 mol) for $x=0.14$, $\gamma \approx 38$ mJ/(K^2 mol) for $x=0.20$, 65.4 mJ/(K^2 mol) for x

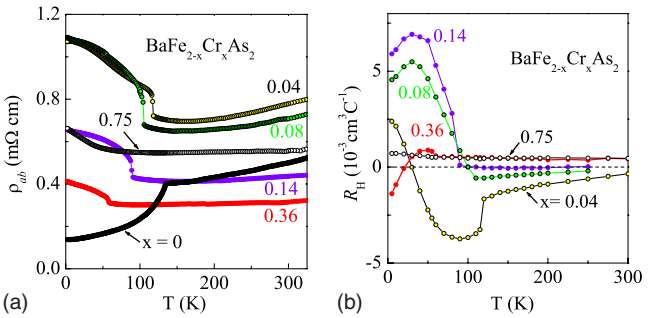

FIG. 3. (Color online) Temperature dependence of (a) resistivity, and (b) Hall coefficient (R_H) for $BaFe_{2-x}Cr_xAs_2$ compositions between $0 \leq x \leq 0.75$, measured in the *ab* plane.

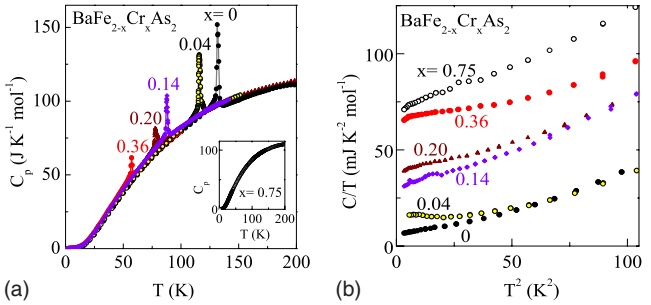

FIG. 4. (Color online) For $BaFe_{2-x}Cr_xAs_2$ and compositions between $0 \leq x \leq 0.75$, temperature dependence of specific heat in (a) $C_p(T)$ form shown below 200 K, and in (b) C_p/T versus T^2 form shown below ~10 K.

=0.36, and largest at ≈70 mJ/(K^2 mol) [or 35 mJ/(K^2 mol transition metal)] for $x=0.75$.

Having both γ and magnetic-susceptibility data, we may further estimate the Wilson ratio $R_w = \pi^2 k_B^2 \chi / (3\mu_B^2 \gamma)$, assuming that $\chi_{spin} \approx \chi$ measured at 1.8 K. For $x=0.14$, R_w is ~5 from χ_{ab} and ~6 from χ_c. For $x=0.20$, R_w is ~6 from χ_{ab} and ~8 from χ_c. For $x=0.36$, R_w is ~9 from χ_{ab} and ~16 from χ_c. Finally for $x=0.75$, R_w is ~13 from χ_{ab} and ~7 from χ_c. These values significantly exceed unity and suggest that $BaFe_2As_2$ approaches ferromagnetism upon Cr doping. We note that the nearness to ferromagnetism and ferromagnetic spin fluctuations are highly destructive to singlet superconductivity, including *s*, *s*+/−, and *d* wave states.

For $BaFe_2As_2$ there is a single sharp peak in C_p consistent with $d(\chi T)/dT$ and $\rho(T)$ results [Fig. 5(a)]. With a small amount of Cr doping, this single sharp peak gives two distinct features in C_p for $x=0.04$ [Fig. 5(b)]: a sharper peak at 115.8 K followed by a shoulder at 118.3 K. From the overlapped data of $\rho(T)$ and $d(\chi T)/dT$, features are observed roughly at the lower-transition temperature, and we assign $T_N \approx 116$ K. As discussed earlier, no detectable symmetry-breaking transition occurs for this composition in single-crystal x-ray diffraction. Therefore the peak-splitting effect in specific heat may be associated with phase separation due to a variation in Cr concentration within the crystal. Among the specific-heat results, $x=0.20$ is the only other composition that gives the double-peak feature [Fig. 5(c)], with $T_N \approx 78$ K and a shoulder at 79 K. Such double-peak splitting has also been seen in the case of Co-doped $BaFe_2As_2$.[13] For $x=0.14$, there is a peak at $T_N \approx 87.5$ K. For $x=0.36$, $T_N \approx 57.3$ K.

Based on the data above, a composition-temperature (x-T) phase diagram is proposed for the hole-doped $BaFe_{2-x}Cr_xAs_2$, shown in Fig. 6. The nature of the magnetic transition temperature for $x \leq 0.36$ is probably of antiferromagnetic SDW type. In order to confirm this, neutron-diffraction studies are in progress. For $x=0.75$, there is probably no magnetic long-range order as there is no λ anomaly in $C_p(T)$, nor a feature in $\rho(T)$. Further investigations are required to explain the feature of ~120 K in $\chi(T)$.

First-principles supercell calculations for $x=1$ were performed within the local density approximation (LDA) with the general potential linearized augmented planewave method (LAPW), similar to those described previously.[10,14] The calculations were done using lattice parameters of $a=3.979$ Å and $c=13.26$ Å. We considered different magnetic orders, specifically, ferromagnetic, LAPW antiferromagnetic (ferromagnetic layers stacked antiferromagnetically along the *c* axis), *G*-type antiferromagnetic (nearest-neighbor antiferromagnetism in all directions, which is the ground state of $BaMn_2As_2$ (Ref. 15) and $BaCr_2As_2$),[10] and a stripe antiferromagnetism, as in the spin-density-wave ground state of $BaFe_2As_2$. We considered three different chemical ordering patterns—a checkerboard ordering of Fe and Cr, with alternation of Fe and Cr along the *c* axis, and a stripe ordering (lines of Fe and Cr neighbors) with both possible stackings along *c*. The atomic positions in the unit cell were separately relaxed for each chemical and magnetic order. The lowest-energy state is for the checkerboard chemical ordering and ferromagnetism. In contrast, with stripe chemical ordering, the lowest-energy state is antiferromagnetic (AFM) with *G*-type ordering. This, however, is 0.10 eV/f.u. higher in energy than the checkerboard chemical ordering. This is a sufficiently high energy that one may expect at least substantial local order in samples grown under the conditions reported here.

Turning to the magnetic properties, we find substantial Fe and Cr magnetic moments independent of chemical order. For the (nonground state) stripe chemical order, we obtained a *G*-type AFM state, with Fe and Cr moments of $1.96\mu_B$ and $2.31\mu_B$, respectively, as defined by the integrals of the spin densities in the LAPW spheres of radius 2.1 Bohr. This state was 0.045 eV lower in energy than the ferromagnetic solution for that chemical ordering. For the low-energy checkerboard chemical order, the ferromagnetic solution is favored over the *G*-type solution by 0.160 eV, which is a very large magnetic energy. Furthermore, the moments are strongly dependent on both chemical and magnetic order. For the lowest-energy ferromagnetic state with checkerboard chemical order, we obtain Fe and Cr moments of $0.97\mu_B$ and $1.80\mu_B$, respectively, while for the *G*-type magnetic order, the Fe and Cr moments become $1.78\mu_B$ and $0.07\mu_B$. On the other hand, the energy difference between the calculated lowest-energy ferromagnetic state and the *A*-type AFM order is very small: 0.003 eV/formula unit indicating rather weak *c*-axis interactions, at least for this chemical order. Also considering the small value of this energy difference and the limitations of density-functional calculations, we cannot ex-

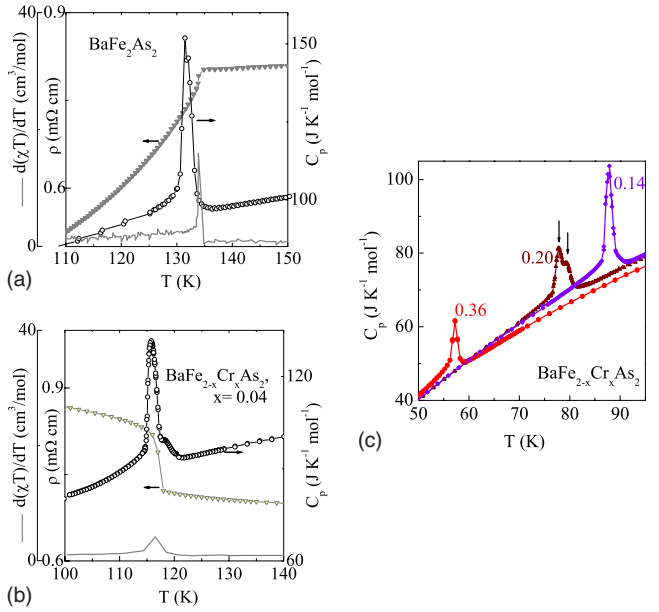

FIG. 5. (Color online) For $BaFe_{2-x}Cr_xAs_2$, the overlapped data of $\rho(T)$, $C_p(T)$, and χ_{ab} shown in the form $d(\chi T)/dT$ for (a) $x=0$ and (b) $x=0.04$. (c) Enlarged $C_p(T)$ region for $x=0.14$, 0.20, and 0.36; the double-peak feature is noted by arrows for $x=0.20$.

clude an A-type AFM ground state. In any case, these results show that there is a very strong interplay between magnetism and chemical ordering in this material, and, based on sensitivity of the magnetic moments to the order, that the magnetism has a strong itinerant component. Finally, we note that the properties of $BaFeCrAs_2$ $(x=1)$ are very different from those of $BaMn_2As_2$, even though the electron count is the same. This is in contrast to the behavior seen in alloys with Fe, Co, and Ni.

We now discuss the ferromagnetic state of chemically ordered $BaFeCrAs_2$ $(x=1)$ in more detail. The calculated band structure, density of states (DOS) and Fermi surface are shown in Figs. 7–9, respectively. The band structure and Fermi surface show a clearly metallic state, with several bands crossing the Fermi energy, and large Fermi surfaces. Furthermore, in conjunction with the projected DOS, one

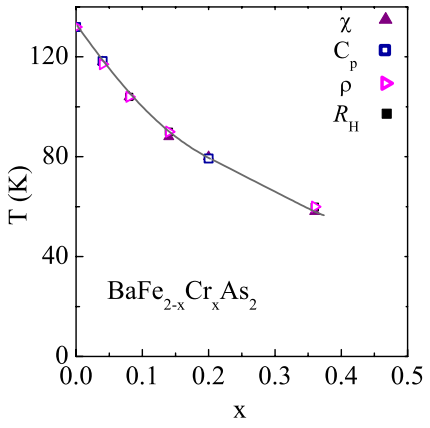

FIG. 6. (Color online) For $BaFe_{2-x}Cr_xAs_2$, magnetic ordering temperature (T_N) versus Cr doping (x).

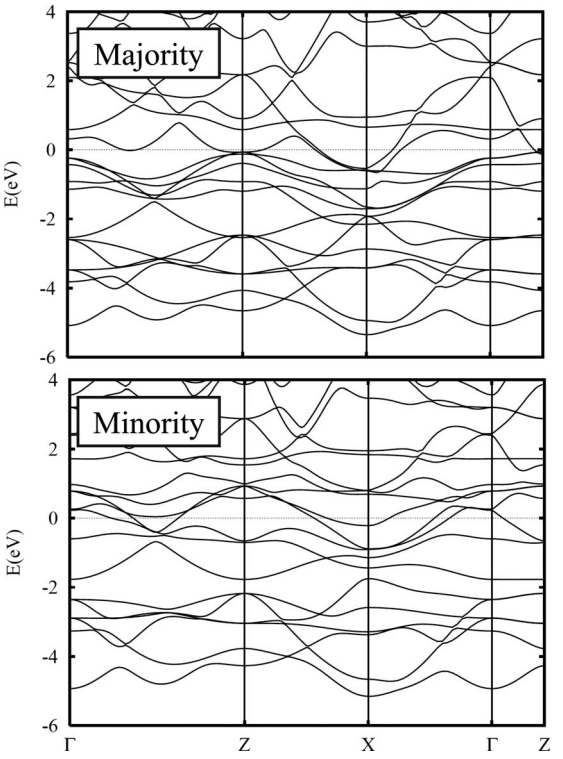

FIG. 7. Calculated majority and minority spin-band structures of checkerboard ordered ferromagnetic $BaFe_{2-x}Cr_xAs_2$ with $x=1$. The directions shown are in the body-centered-tetragonal (bct) basal plane and along the k_z direction, as described in Ref. 12.

may note a strong spin-dependent hybridization, both with As and between the Fe and Cr d orbitals. In particular, one may note that the majority-spin DOS shows very similar coherent shapes of the Fe and Cr contributions, while the minority spin does not. This formation of a coherent metallic majority-spin band structure generally leads to a reduction in band energy and explains why the ferromagnetic ordering is strongly favored. This basic mechanism is closely related to stabilization mechanism for the ferromagnetic metallic state in La rich alloys of $(La,Ca)MnO_3$, for example.[16] In any case, it also provides an explanation of why there is a strong

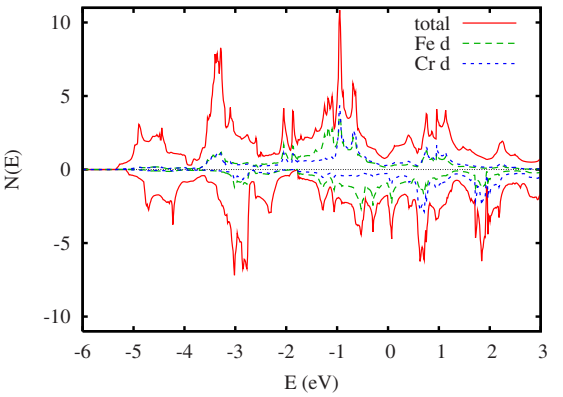

FIG. 8. (Color online) Calculated electronic DOS of ferromagnetic $BaFe_{2-x}Cr_xAs_2$ with $x=1$, on a per formula unit basis. Majority spin is above the axis and minority spin below. The projections are on a per atom basis.

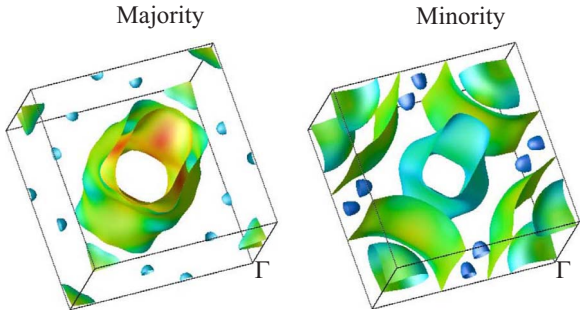

FIG. 9. (Color online) Calculated Fermi surface for majority (left) and minority (right) spin electrons in ordered ferromagnetic $BaFe_{2-x}Cr_xAs_2$ with $x=1$. The shading is by band velocity; light blue represents low-velocity bands and darker green represents high-velocity bands. (Please note the coloring scheme online.)

interplay between chemical and magnetic order. Specifically, with checkerboard chemical order direct nearest-neighbor hopping can only take place between Fe and Cr atoms. This strongly favors a ferromagnetic state, as discussed. On the other hand, for stripelike chemical ordering, the strong covalency between Cr and As, noted previously,[10] provides a strong antiferromagnetic interaction between neighboring Cr atoms and works against a ferromagnetic state, and so an antiferromagnetic state emerges with strongly enhanced moments.

The majority-spin Fermi surface is dominated by two large electron cylinders running along the zone corner and shows additionally small three-dimensional electron sections centered at the Z points (0,0, and 1/2) and some very tiny electron sections. In contrast to the majority spin which is dominated by electron cylinders, the minority-spin Fermi surface shows a prominent multiband character, with a hole cylinder around the zone center and a large electron cylinder around the zone corner. In addition, there are three-dimensional hole pockets around the Γ point and additional tiny hole sections. The DOS at the Fermi energy, $N(E_F)=3.1$ $eV^{-1}/f.u.$ of which 29% comes from the majority spin and the remainder from the minority spin. This corresponds to a bare-band specific-heat $\gamma=7.3$ $mJ/(K^2$ mole f.u.), i.e., 3.65 $mJ/(K^2$ mole transition element). This is much less than measured values for our high Cr content samples, indicating a very strong mass renormalization. The calculated Fermi velocities in the *ab*-plane are 2.3×10^5 m/s and 1.5×10^5 m/s for majority and minority spin, respectively, while the corresponding *c*-axis values are 1.2×10^5 m/s and 0.9×10^5 m/s. These numbers indicate a resistivity anisotropy $\rho_c/\rho_{ab}\sim3$ to 4 depending on the scattering, which may be spin dependent in this material.

Finally, we note that in the Fe-based superconductors there is a general tendency for nonmagnetic LDA calculations to underestimate the height of the As above the Fe planes. This underestimation has been associated with spin fluctuations, which are important in these materials.[17] While it is unclear whether similar physics is applicable in the heavily Cr substituted compounds, we did repeat some of the calculations with the As height arbitrarily increased by 0.15 Å. We find that the lowest-energy state with checkerboard chemical ordering remains ferromagnetic. The Cr moments are rather insensitive to the As height, while the Fe moments increase with As height similar to what was found previously in the pure Fe compounds.[17] In particular, for the lowest-energy ferromagnetic ordering, the Fe moments increase by $0.46\mu_B$ with a 0.15 Å increase in As height.

To summarize the theoretical results, we find a strong interplay between chemical order and magnetic order, a sufficient energy difference between different chemically ordered supercells that we expect local chemical order, and therefore a ferromagnetic tendency in agreement with experiment, and a strong spin-dependent hybridization which may lead to an interesting interplay between transport and magnetic ordering, similar to colossal magnetoresistive manganites.

III. CONCLUSION

As chromium is introduced into FeAs layers in $BaFe_{2-x}Cr_xAs_2$, T_N is suppressed while specific-heat γ increases. The enhanced susceptibilities at $x=0.36$ and $x=75$ levels imply that with increasing x, a ferromagnetic state may be approached. This is consistent with the ferromagnetic ground state that we find for the chemically ordered $x=1$. Considering the strong interplay between chemical order and itinerant magnetic order, as well as the strong spin-dependent hybridization that underlies this, one may expect (1) strong magnetic scattering both because of spin disorder connected with chemical disorder, and also due to spin fluctuations, and (2) the possibility of glassy magnetic behavior in material that is away from the $x=1$ chemical composition and also in material with partial chemical order. In this regard, it will be very interesting to explore the dependence of the properties on stoichiometry for higher Cr contents closer to the $x=1$ composition and also to perform annealing studies to investigate the interplay between magnetic order, transport and chemical order. The present results clearly show a competition between the SDW-type magnetism and another state that is ferromagnetic or very nearly ferromagnetic as Cr is introduced into $BaFe_2As_2$, as well as strong scattering and specific-heat renormalization in the regime where the magnetic crossover occurs. The theoretical results show that ordered $BaFeCrAs_2$ is a rather unusual itinerant ferromagnetic metal with a strong spin-dependent hybridization and an interesting interplay between magnetic and chemical order.

ACKNOWLEDGMENT

The research at ORNL was sponsored by the Division of Materials Sciences and Engineering, Office of Basic Energy Sciences, U.S. Department of Energy.

[1] M. Pfisterer and G. Nagorsen, Z. Naturforsch. B **35B**, 703 (1980).
[2] F. Ronning, T. Klimczuk, E. D. Bauer, H. Volz, and J. D. Thompson, J. Phys.: Condens. Matter **20**, 322201 (2008).
[3] C. Krellner, N. Caroca-Canales, A. Jesche, H. Rosner, A. Ormeci, and C. Geibel, Phys. Rev. B **78**, 100504(R) (2008).
[4] M. Rotter, M. Tegel, D. Johrendt, I. Schellenberg, W. Hermes, and R. Pottgen, Phys. Rev. B **78**, 020503(R) (2008).
[5] A. S. Sefat, M. A. McGuire, R. Jin, B. C. Sales, D. Mandrus, F. Ronning, E. D. Bauer, and Y. Mozharivskyj, Phys. Rev. B **79**, 094508 (2009).
[6] Z. Ren, Z. W. Zhu, S. A. Jiang, X. F. Xu, Q. Tao, C. Wang, C. M. Feng, G. H. Cao, and Z. A. Xu, Phys. Rev. B **78**, 052501 (2008).
[7] M. Gooch, B. Lv, B. Lorenz, A. M. Guloy, and C. W. Chu, Phys. Rev. B **78**, 180508(R) (2008).
[8] M. Rotter, M. Tegel, and D. Johrendt, Phys. Rev. Lett. **101**, 107006 (2008).
[9] A. S. Sefat, R. Jin, M. A. McGuire, B. C. Sales, D. J. Singh, and D. Mandrus, Phys. Rev. Lett. **101**, 117004 (2008).
[10] D. Singh, A. Sefat, M. McGuire, B. Sales, D. Mandrus, L. VanBebber, and V. Keppens, Phys. Rev. B **79**, 094429 (2009).
[11] J. Rodriguez-Carvajal, FULLPROF Suite 2005, version 3.30, ILL, 2005.
[12] A. S. Sefat, D. J. Singh, R. Jin, M. A. McGuire, B. C. Sales, and D. Mandrus, Phys. Rev. B **79**, 024512 (2009).
[13] J. H. Chu, J. G. Analytis, C. Kucharczyk, and I. R. Fisher, Phys. Rev. B **79**, 014506 (2009).
[14] D. J. Singh and L. Nordstrom, *Planewaves Pseudopotentials and the LAPW Method*, 2nd ed. (Springer, Berlin, 2006).
[15] J. An, A. S. Sefat, D. J. Singh, and M. H. Du, Phys. Rev. B **79**, 075120 (2009).
[16] W. E. Pickett and D. J. Singh, Phys. Rev. B **53**, 1146 (1996).
[17] I. I. Mazin, M. D. Johannes, L. Boeri, K. Koepernik, and D. J. Singh, Phys. Rev. B **78**, 085104 (2008).